

# Sensitive and Stretchable Strain Sensors Based on Silver Nanowires Network

W. G. Song<sup>1,†</sup>, S. Yun<sup>2,†</sup>, K. Kyung<sup>2,†</sup>, M. Kim<sup>1</sup>, J. Lee<sup>1</sup>, J. Baek<sup>1</sup>, S. Kim<sup>1,\*</sup>, and Y. K. Hong<sup>1,\*</sup>

<sup>1</sup>Department of Electronic and Radio Engineering, Kyung Hee University, Youngin 446-701, Korea

<sup>2</sup>Transparent Transducer and UX Creative Research Center, Electronics and Telecommunication Research Institute, Daejeon 305-700, Korea

In this paper, we report on mechanical and electrical properties of the stretchable strain sensor based on two-dimensional network of silver nanowires embedded between bio-compatible polydimethylsiloxane films. Our strain sensor shows a quasi-linear response of resistance change with respect to stretching up to 15%. Dynamic stability and durability of the strain sensor are investigated through cyclic stretching test (1,000 times). We also demonstrate sensitivity of our strain sensor under the pulse-type stresses with arbitrary intensities.

**Keywords:** Flexible Electronics, Stretchable Sensor, Strain, Silver Nanowire.

## 1. INTRODUCTION

Various flexible sensors targeting into pressure, strain, touch, and optical signals have received considerable attentions due to their versatile applications, such as personal health monitoring,<sup>1,2</sup> wearable electronic skin,<sup>3,4</sup> and human motion capturing.<sup>5</sup> Among them, strain sensors by using carbon nanotubes,<sup>6-8</sup> graphenes,<sup>9-11</sup> and metal nanostructures<sup>12,13</sup> have been developed as flexible detectors for change of electrical characteristics of sensing layer under various mechanical stresses due to their outstanding electrical and mechanical properties.<sup>14,15</sup> In particular, sensitivity and stretchability of strain sensor are main issues to interact and detect mechanical deformation within human body.<sup>16,17</sup> However, several drawbacks, for examples, poor detectability of strain (minimum  $\varepsilon = 2.47\%$ ),<sup>18</sup> low sensitivity gauge factor and stretchability, nonlinearity, and large hysteresis<sup>5,14,15</sup> have limited their industrial applications.<sup>19-21</sup>

Recently, two-dimensional (2D) network based on metal nanowires (NWs) have been spotlighted as emerging candidates for next generation strain sensing layers.<sup>22,23</sup> Silver (Ag) NWs network is one of the most successful flexible sensing layer owing to its optical, electrical, and mechanical properties.<sup>24,25</sup> However, it has been known that Ag NWs exhibited a weak adhesion on flexible

polymer substrate, resulting in the degradation of their electric properties under the stress application due to the repetitive stretching and releasing.<sup>22,26,27</sup>

In this paper, we demonstrate flexible strain sensors fabricated by using 2D network of Ag NWs embedded between bio-compatible polydimethylsiloxane (PDMS) films. The variations of the electrical properties of our strain sensors are investigated under various mechanical stresses, which show excellent performances with a high linearity and mechanical stability under the cyclic and static condition of stretching and releasing. We also demonstrate sensitivity of our strain sensor under the pulse-type stresses with arbitrary intensities.

## 2. EXPERIMENTAL DETAILS

Figure 1(a) showed the fabricating procedure of flexible strain sensor. PDMS (Sylgard 184, Dow Corning) was mixing with the base and the curing agent (typically at 10:1 wt%). The mixture was spin-coated on glass substrate, and placed in an oven to cure at 90 °C for 15 min (PDMS1 layer).

The Ag NWs, fabricated through the polyol method,<sup>28</sup> were homogeneously dispersed in isopropyl alcohol (IPA) with a concentration of 0.5 wt% (Nanopyxis, South Korea). The Ag NWs/IPA solution was further diluted to be a concentration of 0.1 wt%, and spray-coated onto the PDMS1/glass substrate. After drying residual solvent at room temperature (RT) for at least 2 hours, copper wires

\*Authors to whom correspondence should be addressed.

†These three authors contributed equally as co-first authors.

were connected to both ends of Ag NWs network by using conductive paste. Then, PDMS2 layer was cast on top of the Ag NWs/PDMS1 substrate, followed by curing at 70 °C for 20 min. Finally, free standing structure of PDMS2/Ag NWs/PDMS1 film was obtained through the gentle detachment from glass substrate.

Dimensions of individual NWs and their 2D network structure were investigated by using scanning electron microscope (SEM, FEI SIRION 400) without PDMS2 layer. For applying stresses originated from stretching/releasing, the strain sensor (PDMS2/Ag NWs/PDMS1) was mounted on a moving stage, and electrical properties were measured by using the semiconductor characterization system (Keithley-4200-SCS) at RT under atmospheric environments.

### 3. RESULTS AND DISCUSSION

Figure 1 presents that our strain sensor has a sandwich-structure, in which Ag NWs were intercalated one another between PDMS layers. As shown in Figure 1(c), average diameter and length of the Ag NWs were estimated to 25 ( $\pm 5$ ) nm and 35 ( $\pm 5$ )  $\mu\text{m}$ , respectively, which were interconnected to form 2D network structure. PDMS is an elastomeric material that has large nonlinear elastic deformation. When the strain is released, buckling and fracture emerge at the interface of Ag NWs and PDMS layer because of the difference of mechanical properties and weak adhesion between them. In order to minimize these effects, we piled the PDMS2 on Ag NWs/PDMS1 for establishing the sandwich-structured strain sensor. When the PDMS solution is cast on the Ag NWs/PDMS1 substrate, it could permeate into the empty space between the each Ag NW due to its low viscosity and surface energy.<sup>26</sup>

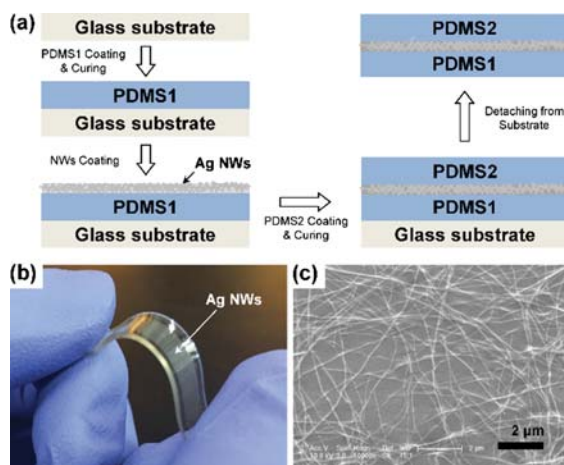


**Figure 1.** (a) Schematic procedure for the fabrication of strain sensor based on Ag NWs and PDMS films. (b) Photograph of the strain sensor under bending. (c) SEM image of Ag NWs network on surface of PDMS1.

As a result, the Ag NWs were embedded in PDMS2, in which the initial positions of Ag NWs and their corresponding contacts were supported against stretching. These “embedded sandwich-structure” provides that our strain sensors have stable and robust sensing capability even under the repetitive stretch/release cycle. In addition, the sandwich structure also acts as protective layers against oxygen/moisture exposure as well as mechanical stimuli on the surface under harsh environments.

Figure 2(a) shows photographs of the pristine (i.e., non-stretched) and stretched strain sensor with various strains ( $\epsilon = 0, 15,$  and 50%), which defined as the ratio of length variation to its original dimension under the elongation of the device. Note that dimensions and shape of our sensor were well recovered to its initial state even after 50% elongation. Figure 2(b) compares the current–voltage ( $I$ – $V$ ) characteristics of the pristine and stretched sensor under different static strains. The  $I$ – $V$  characteristics of the pristine sensor exhibits an Ohmic behavior, and resistance calculated from the slope is 375  $\Omega$ . As increasing  $\epsilon$ , the current levels of the stretched sensor gradually decreased, and the nonlinearity of the  $I$ – $V$  curves began to be observed. Figure 2(c) presents resistance variation of the strain sensor as a function of the static  $\epsilon$ . When  $\epsilon$  was varied between 0 and 15.6% (black squares), resistance at each static  $\epsilon$  exhibits a quasi-linear response in semi-logarithmic scale, and very little hysteresis was observed,

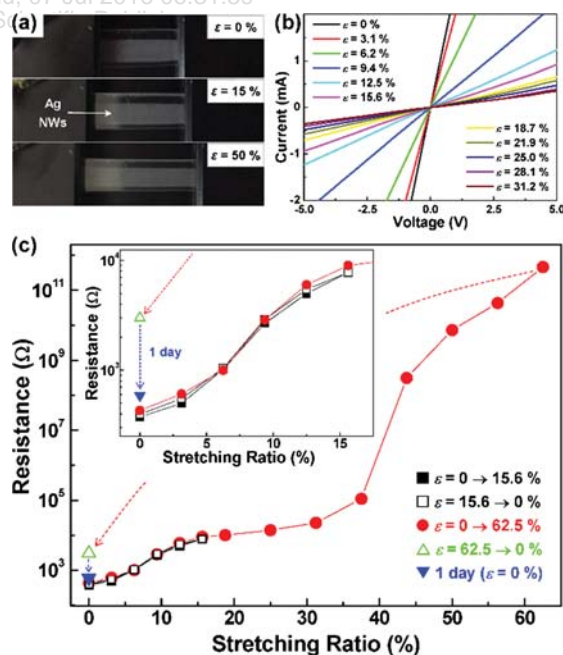


**Figure 2.** (a) Photographs of the pristine and stretched strain sensors up to 50% elongation. (b) Comparison of the  $I$ – $V$  characteristics of strain sensor under the different levels of strains. (c) Variation of resistance as a function of the static strain. Inset: Magnification of (c) in relatively low strain region.

as also shown in the inset of Figure 2(c). It should be noted that this resistance variation was highly reproducible under the multiple repetition of the static stretching–releasing ( $\varepsilon$ :  $0 \rightleftharpoons 15.6\%$ ). As increasing  $\varepsilon$  up to  $62.5\%$ , resistance of the stretched sensor was abruptly enhanced after about  $40\%$  of  $\varepsilon$ , and hysteresis behavior became significantly severe. After  $\varepsilon$  was reduced to  $0$ , resistance of the sensor was changed from  $464 \text{ G}\Omega$  ( $\varepsilon = 62.5\%$ ) to  $3.0 \text{ k}\Omega$  ( $\varepsilon = 0$ ), which was further relaxed to  $591 \Omega$  in 24 hours. However, resistance at  $\varepsilon = 0$  did not return to its original value, as shown in Figure 2(c). Based on above discussion, a confidential dynamic range of our strain sensor could be suggested up to  $15\%$  of  $\varepsilon$ .

Figure 3 presents the performances of our strain sensor under the repetitive applications of stretching–releasing cycles with uniform intensities. As shown in Figure 3(a), the resistance variation of the strain sensor was monitored up to 1,000 cycles ( $\varepsilon = 5\%$ ), which was maintained less than  $13.7\%$  ( $\pm 2.75\%$ ). It should be noted that the resistance after finishing each number of cyclic stretching was measured at non-stretched condition. The stable responses of our device against cyclic stretching indicated reasonable stability and durability of the sensing performance. Based on these result, the strain sensor after repetitive mechanical

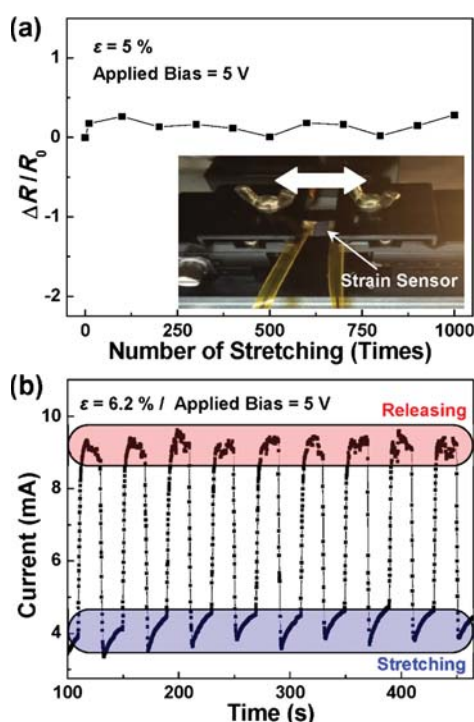


**Figure 3.** (a) Resistance variation of the strain sensor under the cyclic stretching test ( $\varepsilon = 5.0\%$ ) with respect to the number of stretching. Inset: Photograph of cyclic stretching test by using moving stage. (b)  $I-t$  characteristics of the strain sensor under the periodic applications of stretching (release)-duration cycles with uniform strain intensity ( $\varepsilon = 6.2\%$ ).

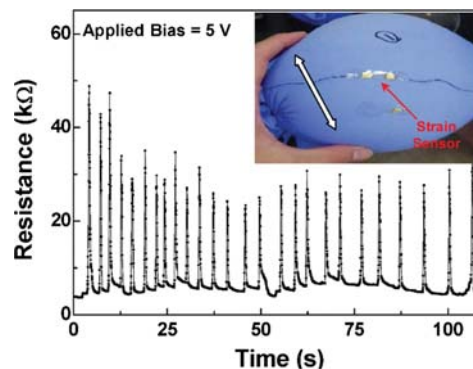


**Figure 4.**  $R-t$  characteristics of the strain sensor under pulse-type stresses with arbitrary intensities. Inset: strain sensor attached onto the surface of balloon.

deformation was proved to be highly steady under stretch–release cycles. Figure 3(b) shows the current–time ( $I-t$ ) characteristic behavior of the strain sensor under the periodic applications of stretching–duration–releasing–duration cycles, in which each stretching/releasing and duration times were controlled  $\sim 1 \text{ s}$  and  $20 \text{ s}$ , respectively. Current level was logarithmically increased within each stretched region, where the constant strain was maintained ( $\varepsilon = 6.2\%$ ). The result could be attributed to the initial degradation and stabilization of the mechanical contact-points among Ag NWs, originated from the initial movements of individual NWs due to the quick stretching procedure.<sup>15</sup> The enhancement, duration, and recovery of current levels were well observed, corresponding to their counterparts in the multiple stretching (releasing)-duration cycles. This result could imply the potentials of our strain sensor to the field of motion-detecting application.

In order to further investigate the responsivity of our strain sensor in terms of speed and intensity, it was attached onto the surface of balloon, and pulse-type stresses with arbitrary intensities were applied through squeezing the balloon by hand (see the inset of Fig. 4). The resistance–time ( $R-t$ ) characteristic behavior of our sensor shows a highly sensitive and fast responsive nature, which reflects the expansion/contraction of the sensor-attached area in balloon, as shown in Figure 4. In addition, gradual reduction of resistance in each stress released region might be originated from a delayed response of the elastomeric PDMS in terms of mechanical deformation and resilience.<sup>15, 26</sup>

#### 4. CONCLUSION

We successfully fabricated highly sensitive and stretchable strain sensor based on 2D network of Ag NWs and bio-compatible PDMS layers. The strain sensor with embedded sandwich-structure showed outstanding performances in terms of linearity, sensitivity, stability, and fast response

under relatively wide range of strain. Static and cyclic modes of stretching test also guaranteed our strain sensor to the various applications, which should require high performances of sensing capabilities.

**Acknowledgment:** This research was supported in part by the National Research Foundation of Korea (NRF-2013M3C1A3059590, NRF-2014M3A9D7070732, and 2012R1A1A1042630) and the Commercializations Promotion Agency for R&D Outcomes (COMPA) funded by the Ministry of Science, ICT and Future Planning (MISP).

### References and Notes

1. D. H. Kim and J. A. Rogers, *Adv. Mater.* 20, 4887 (2008).
2. G. Schwartz, B. C. K. Tee, J. Mei, A. L. Appleton, D. H. Kim, H. Wang, and Z. Bao, *Nat. Commun.* 4, 1859 (2013).
3. D.-H. Kim, N. Lu, R. Ma, Y.-S. Kim, R.-H. Kim, S. Wang, J. Wu, S. M. Won, H. Tao, and A. Islam, *Science* 333, 838 (2011).
4. M. L. Hammock, A. Chortos, B. C. K. Tee, J. B. H. Tok, and Z. Bao, *Adv. Mater.* 25, 5997 (2013).
5. N. Lu, C. Lu, S. Yang, and J. Rogers, *Adv. Funct. Mater.* 22, 4044 (2012).
6. I. Kang, K. Y. Joung, G. R. Choi, M. J. Schulz, Y. S. Choi, S. H. Hwang, and H. S. Ko, *J. Nanosci. Nanotechnol.* 7, 3736 (2007).
7. K. J. Loh, J. Kim, J. P. Lynch, N. W. S. Kam, and N. A. Kotov, *Smart Mater. Struct.* 16, 429 (2007).
8. D. J. Lipomi, M. Vosguerichian, B. C. K. Tee, S. L. Hellstrom, J. A. Lee, C. H. Fox, and Z. Bao, *Nature Nanotech.* 6, 788 (2011).
9. E. W. Hill, A. Vijayaraghavan, and K. Novoselov, *IEEE Sens. J.* 11, 3161 (2011).
10. S. B. Kumar and J. Guo, *Nano Lett.* 12, 1362 (2012).
11. Y. Wang, R. Yang, Z. Shi, L. Zhang, D. Shi, E. Wang, and G. Zhang, *ACS Nano* 5, 3645 (2011).
12. H. Wu, L. Hu, M. W. Rowell, D. Kong, J. J. Cha, J. R. McDonough, J. Zhu, Y. Yang, M. D. McGehee, and Y. Cui, *Nano Lett.* 10, 4242 (2010).
13. Y. Xia, P. Yang, Y. Sun, Y. Wu, B. Mayers, B. Gates, Y. Yin, F. Kim, and H. Yan, *Adv. Mater.* 15, 353 (2003).
14. S. H. Bae, Y. Lee, B. K. Sharma, H. J. Lee, J. H. Kim, and J. H. Ahn, *Carbon* 51, 236 (2013).
15. M. Amjadi, A. Pichitpajongkit, S. Lee, S. Ryu, and I. Park, *ACS Nano* 8, 5154 (2014).
16. Z. Cui, F. R. Pobleto, G. Cheng, S. Yao, X. Jiang, and Y. Zhu, *J. Mater. Res.* 30, 79 (2015).
17. T. Q. Trung, N. T. Tien, D. Kim, M. Jang, O. J. Yoon, and N. E. Lee, *Adv. Funct. Mater.* 24, 117 (2014).
18. X.-W. Fu, Z.-M. Liao, J.-X. Zhou, Y.-B. Zhou, H.-C. Wu, R. Zhang, G. Jing, J. Xu, X. Wu, and W. Guo, *Appl. Phys. Lett.* 99, 213107 (2011).
19. M. Hempel, D. Nezhich, J. Kong, and M. Hofmann, *Nano Lett.* 12, 5714 (2012).
20. X. Li, R. Zhang, W. Yu, K. Wang, J. Wei, D. Wu, A. Cao, Z. Li, Y. Cheng, and Q. Zheng, *Sci. Rep.* 2, 870 (2012).
21. D. J. Cohen, D. Mitra, K. Peterson, and M. M. Mahabiz, *Nano Lett.* 12, 1821 (2012).
22. F. Xu, J. W. Durham III, B. J. Wiley, and Y. Zhu, *ACS Nano* 5, 1556 (2011).
23. W. Lu and C. M. Lieber, *J. Phys. D: Appl. Phys.* 39, R387 (2006).
24. D. S. Hecht, L. Hu, and G. Irvin, *Adv. Mater.* 23, 1482 (2011).
25. X. Y. Zeng, Q. K. Zhang, R. M. Yu, and C. Z. Lu, *Adv. Mater.* 22, 4484 (2010).
26. F. Xu and Y. Zhu, *Adv. Mater.* 24, 5117 (2012).
27. S. De, T. M. Higgins, P. E. Lyons, E. M. Doherty, P. N. Nirmalraj, W. J. Blau, J. J. Boland, and J. N. Coleman, *ACS Nano* 3, 1767 (2009).
28. J. W. Kim, S. W. Lee, Y. Lee, S. B. Jung, S. J. Hong, and M. G. Kwak, *J. Nanosci. Nanotechnol.* 13, 6244 (2013).

Received: 19 June 2015. Accepted: 7 August 2015.